Methods

Chemical synthesis. All reagents and solvents were purchased from Sigma-Aldrich (Bornem, Belgium), Acros (Geel, Belgium) or Fluka (Bornem, Belgium) and were used without further purification. ^{1}H-NMR spectra were recorded on a Bruker AVANCE 300 MHz spectrometer (Bruker AG, Faellanden, Switzerland) using DMSO-d_6 as solvent. Chemical shifts are reported in parts per million relative to tetramethylsilane (δ = 0). Coupling constants are reported in hertz. Splitting patterns are defined by s (singlet), d (doublet), dd (double doublet), t (triplet) or m (multiplet).

Mass measurements were performed on a time-of-flight mass spectrometer (LCT, Micromass, Manchester, UK) equipped with an orthogonal electrospray ionization (ESI) interface. Acquisition and processing of data was done using Masslynx software (version 3.5, Micromass).

(*2,3-Dichlorophenyl)-[5-methoxy-2-methyl-3-(2-morpholin-4-yl-ethyl)-indol-1-yl]-methanone* (reference product, GW405833))

Synthesis of GW405833 was performed according to literature methods yielding a yellow solid (yield = 61 %) (*1*). TLC: R_f = 0.6 (dichloromethane with 3 % CH_3OH) or R_f = 0.8 (dichloromethane with 5 % CH_3OH). HPLC (XBridge RP18 column 5 µm, 4.6 mm x 150 mm, Waters; EtOH/NH_4OAc 0.05 M pH 6.9 60/40; 1 ml/min): t_R = 5.4 min (99 %). ^{1}H NMR (DMSO) δ 7.899 (1H, D, $^{3}J_{H\text{-}H}$ = 8.0 Hz, 4-H_{ar}), 7.704 (1H, D, $^{3}J_{H\text{-}H}$ = 7.0 Hz, 6-H_{ar}), 7.587 (1H, t, $^{3}J_{H\text{-}H}$ = 7.8 Hz, 5-H_{ar}), 7.365 (1H, D, $^{3}J_{H\text{-}H}$ = 8.5, 7-H), 7.031 (1H, d, $^{4}J_{H\text{-}H}$ = 2.3 Hz, 4-H), 6.791 (1H, dD, $^{3}J_{H\text{-}H}$ = 9.0 Hz and $^{4}J_{H\text{-}H}$ = 2.3 Hz, 6-H), 3.796 (3H, s, OCH_3), 3.574 (4H, t, $^{3}J_{H\text{-}H}$ = 4.4 Hz, 2 x $NCH_2\underline{CH_2}O$), 2.766 (2H, t, $^{3}J_{H\text{-}H}$ = 7.6 Hz, $\underline{CH_2}CH_2N$), 2.445 - 2.406 (6H, m, $CH_2\underline{CH_2}N$ and 2 x $N\underline{CH_2}CH_2O$), 2.014 (3H, s, 2-CH_3).

(*2,3-Dichlorophenyl)-[5-hydroxy-2-methyl-3-(2-morpholin-4-yl-ethyl)-indol-1-yl]-methanone* (precursor for labelling, **1**)

To a stirred solution of (2,3-dichloro-phenyl)-[5-methoxy-2-methyl-3-(2-morpholin-4-yl-ethyl)-indol-1-yl]-methanone (GW405833) (0.320 g, 0.715 mmol) in dry dichloromethane (10 ml) under nitrogen at -70 °C a 1 M solution of boron tribromide in dichloromethane (2.9 ml) was added dropwise over 30-45 min. The mixture was maintained at -70 °C for 1 h and then allowed to warm slowly to room temperature after which the mixture was stirred overnight. The reaction mixture was again cooled to -70 °C and the excess of boron tribromide was quenched by dropwise addition of methanol until no further reaction occurred. The reaction mixture was purified by column chromatography on silica gel (63-200 µm particle size, 60 Å, MPBiomedicals, Eschwege, Germany) using dichloromethane-methanol (gradient 0 to 5 % methanol) as the eluent yielding a yellow-white solid (0.192 g, yield = 62 %). TLC: R_f = 0.6 (dichloromethane with 5 % CH_3OH). HPLC (XTerra RP18 column 5 µm, 4.6 mm x 250 mm, Waters; CH_3CN/NH_4OAc 0.05 M pH 6.9 60/40; 1 ml/min): t_R = 6.1 min (98 %). ^{1}H NMR (DMSO) δ 9.315 (1H, s, 5-OH), 7.881 (1H, dD, $^3J_{H\text{-}H}$ = 8.0 Hz and $^4J_{H\text{-}H}$ = 1.4 Hz, 4-H_{ar}), 7.672 (1H, dD, $^3J_{H\text{-}H}$ = 7.6 Hz and $^4J_{H\text{-}H}$ = 1.4 Hz, 6-H_{ar}), 7.567 (1H, t, $^3J_{H\text{-}H}$ = 7.8 Hz, 5-H_{ar}), 7.325 (1H, D, $^3J_{H\text{-}H}$ = 8.1 Hz, 7-H), 6.833 (1H, d, $^4J_{H\text{-}H}$ = 2.3 Hz, 4-H), 6.622 (1H, dD, $^3J_{H\text{-}H}$ = 8.9 Hz and $^4J_{H\text{-}H}$ = 2.3 Hz, 6-H), 3.575 (4H, t, 2 x $NCH_2\underline{CH_2}O$), 2.700 (2H, t, $\underline{CH_2}CH_2N$), 2.434-2.365 (6H, m, $CH_2\underline{CH_2}N$ and 2 x $N\underline{CH_2}CH_2O$), 1.966 (3H, s, 2-CH_3). MS $(ES)^+$ Accurate mass: $[C_{22}H_{22}Cl_2N_2O_3 + H]^+$ theoretical mass 433.1080 Da and found 433.1070 Da.

Radiosynthesis

Synthesis of [^{11}C]CH_3I and [^{11}C]GW405833

[^{11}C]CH_3I was produced according to methods described by Larsen et al.(*2*). [^{11}C]CH_3I was used as such or passed through a column (150 mm x 3 mm) filled with silver triflate (50 mm silver triflate between two times 50 mm quartz wool) heated to 180 °C, yielding the more reactive [^{11}C]methyl triflate. A stream of helium containing the alkylating agent was bubbled through a solution of 200 µg **1** and 2-4 mg Cs_2CO_3 in 200 µl DMF. The reaction mixture was heated during 2 min at 90 °C, diluted with 1.8 ml 0.05 M ammonium acetate buffer pH 6.9 containing 30 % ethanol and applied onto an XBridge RP18 column (5

μm, 4.6 mm x 150 mm; Waters) which was eluted with 0.05 M ammonium acetate buffer (pH = 6.9)/EtOH (50:50 v/v, 1 ml/min).

Quality control

Quality control for [^{11}C]GW405855 using authentic GW405833 as a reference was done by HPLC on an XTerra RP18 column (5 μm, 4.6 mm × 250 mm, Waters) eluted with 0.05 M ammonium acetate buffer pH 6.9/acetonitrile (40:60 v/v, 1 ml/min).

Distribution coefficient. Determination of the distribution coefficient of [^{11}C]GW405833 by partitioning between 1-octanol and 0.025 M phosphate buffer pH 7.4 was done according to a previously described method (*3*).

Biodistribution studies in mouse and rat. Quantification of radioactivity for biodistribution and radiometabolite studies was done using a gamma counter (3-inch NaI(Tl) well crystal) coupled to a multi-channel analyzer and mounted in a sample changer (Wallac 1480 Wizard® 3", Wallac, Turku, Finland). The values were corrected for background radiation and physical decay during counting. All biodistribution studies were conducted in male NMRI mice (37-50 g, n=4) and male Wistar rats (203-234 g, n=3). Mice and rats were anesthetized with isoflurane (2 % in oxygen). The solution of the HPLC purified product was diluted with saline to a concentration of approximately 50 MBq/ml and an ethanol concentration ≤ 10 %. An aliquot of 100 or 300 μl (for mice or rats respectively) was injected via a tail vein. The animals were sacrificed by decapitation and the organs and body parts were dissected and weighed. Radioactivity in the dissected organs and blood was measured using a gamma counter. For calculation of total blood radioactivity, blood mass was assumed to be 7 % of the body mass (*4*).

Viral vector construction and production. A LV transfer plasmid was constructed encoding hCB_2 harboring a point mutation at position 80 (D80N) and referred to as hCB_2(D80N). The hCB_2(D80N) cDNA sequence was amplified by PCR using as a template pcDNA3 hCB_2(D80N) (provided by Dr. Mary

E. Abood, Virginia Commonwealth University, USA) and as primers CB_2 forward (5'-GAGCTCGGATCCATGGAGGAATGCTGGGTGACAG-3') and CB_2 reverse (5'-CCCGGGCTCGAGTCAGCAATCAGAGAGGTCTAGATCTCTG-3'). The amplified product was digested with BamHI and XhoI, and further subcloned in BamHI-XhoI sites of the transfer plasmid pCHMWS (*5*), yielding pCHMWS-hCB_2(D80N) (LV-hCB_2(D80N)). Two bicistronic LV were constructed encoding either hCB_2(D80N) and eGFP, or hCB_2(D80N) and hygromycin B phosphotransferase separated by an EMCV IRES sequence (*6*). Highly concentrated LV were produced as described previously (*7*). Filtered vector particles were concentrated using Vivaspin15 columns (Vivascience, Hannover, Germany), aliquoted and stored at -80°C until use. For transduction experiments HEK-293T cells were seeded in a 96-well plate at 20,000 cells per well. The next day, the cells were transduced with vector preparations serially diluted in DMEM supplemented with 10% FCS. After 6 hours of incubation, the vectors were washed from the cells and medium was replaced. Cells were passaged (1/10) at least 4 times to exclude pseudo-transduction. Stably transduced cells were seeded in quadruplet in 96-well plates at 1.5 x 10^4 cells per cup in 200 µl DMEM with 10% FCS and used in the different experimental settings.

To clone hCB_2(D80N) in the AAV transfer plasmid, the LV pCHMWS- hCB_2(D80N) plasmid was first digested with BamHI and MluI. The hCB_2(D80N) coding sequence was then ligated downstream of the hCMVie promoter into the BamHI and MluI linearized AAV transfer plasmid (*8*), but before the WPRE (*9*) and the bovine growth hormone polyadenylation (BGH polyA) signal. In parallel a bicistronic AAV transfer plasmid was constructed encoding the hCB_2(D80N) transgene in combination with eGFP or firefly luciferase making use of T2A (*10,11*). AAV vector productions were performed with a protocol similar to that of the LV productions. Briefly, HEK-293T cells were plated in 10 cm petri dishes in OPTIMEM with 2 % FCS. The following day a transient transfection was carried out using polyethylene-imine (PEI) with the AAV transfer plasmid containing either the eGFP-T2A-hCB_2(D80N) or the Fluc-T2A-hCB_2(D80N) as transgenes, the AAV serotype 7 plasmid (pAAV2/7) (*8*) and the AAV helper plasmid. Subsequently the cells were grown under serum free conditions. The supernatant was collected

after 48 hours and concentrated using centrifugal concentrators (Vivaspin, Sartorius) with a 50,000 Dalton cut-off. Viral titers were determined as DNase resistant genome copies using a standard qPCR (*8*).

Cell culture and transduction. HEK (human embryonic kidney)-293T cells and SHSY5Y (human dopaminergic neuroblastoma) cells were maintained in Dulbecco's modified Eagle's medium (DMEM) with Glutamax (Gibco BRL, Invitrogen, Merelbeke, Belgium) supplemented with 10 % heat-inactivated foetal calf serum (Harlan Sera-Lab Ltd., International Medical, Brussels, Belgium) and 1 % penicillin (10,000 U/ml)/streptomycin (10 mg/ml) (Gibco BRL). Cells were cultured at 37 °C in a humidified atmosphere containing 5 % CO_2. The day before transduction, cells were seeded in a 24-well plate at 100,000 cells per well. The cells were transduced during 24 h before the medium was replaced.

Western blot analysis. Extracts of HEK-293T transduced cells were made using 1 % SDS complemented with CompleteTM protease inhibitors (Roche Diagnostics GmbH, Mannheim, Germany). 10 µg of total protein (heated/non-heated for 1 min at 100 °C) was separated in a self-cast 12.5 % SDS-polyacrylamide gel and transferred to a polyvinylidenedifluoride (PVDF) membrane (Bio-Rad, Watford, United Kingdom). The PVDF membrane was incubated overnight at 4 °C in PBS containing 0.1 % Tween20 and 5 % milk powder and then at room temperature for 2 h with a polyclonal primary antibody against CB_2 (Cayman Chemical, Michigan, USA) at a dilution of 1:1,000. After washing in PBS + 0.1 % Tween20 (3x10 min), the blot was incubated at room temperature for 1 h with horseradish peroxidase (HRP)-conjugated anti-rabbit secondary antibody. The blot was washed in PBS + 0.1 % Tween20 (3x10 min) and immunoreactive proteins were visualized using the enhanced chemiluminescence plus (ECL^+) kit (Amersham Biosciences, Uppsala, Sweden).

Stereotactic injections of viral vectors. 8-10 week old adult female Wistar and Fisher rats were used. The animals were housed under 14h light/10 h dark cycle with free access to food and water. Studies were performed in accordance with the current institutional regulations for use and care of laboratory animals

provided by the University of Leuven (P067/2009). Animals were anesthetized intraperitoneally with ketamine (75 mg/kg; Ketalar, Pfizer, Brussels, Belgium) and medetomidin (1 mg/kg; Domitor, Pfizer), and positioned in a stereotactic head frame (Stoelting, Wood Dale, IL, USA). Using a 30-gauge needle on a 10 µl Hamilton syringe 5 µl was injected at a rate of 0.25 µl/ min. The coordinates used for striatal injection of the CB_2 vectors (LV-hCB_2(D80N), AAV-eGFP-T2A-hCB_2(D80N) or AAV-Fluc-T2A-hCB_2(D80N)) were anteroposterior 0 cm, lateral -0,28 cm and dorsoventral -0,55 cm relative to bregma. The coordinates used for striatal injection of the control vector AAV-eGFP-T2A-Fluc were anteroposterior 0 cm, lateral +0,28 cm and dorsoventral -0,55 cm relative to bregma. After 10 min of injection (2.5 µl), the needle was raised slowly in the dorsal direction until -0.45 cm relative to bregma. After surgery anaesthesia was reversed with an intraperitoneal injection of atipamezol (0.5 mg/kg; Antisedan, Orion Pharma, Newbury, Berkshire, UK).

Bioluminescence imaging. Three Fisher rats were stereotactically injected with AAV-Fluc-T2A-hCB_2(D80N) in the right striatum and received a BLI scan at 16, 58 and 281 days after surgery (alternated with µPET). Rats were imaged using the IVIS 100 system (Xenogen, Alameda, CA, USA). Anesthesia was induced in an induction chamber with 2.5 % isoflurane in 100 % oxygen at a flow rate of 1 l/min and maintained in the IVIS with a 2 % mixture at 0.5 % l/min. Before each imaging session rats were injected intravenously with 126 mg/kg D-luciferin (Xenogen, Teralfene, Belgium) dissolved in PBS (30 mg/ml). Consecutive 1 min frames were acquired until the maximum signal was reached. Data are represented as the maximum pixel (p/s/cm^2/sr) of a region of interest.

Immunofluorescence and immunohistochemistry. Rats were sacrificed with an intraperitoneal injection of pentobarbital followed by a transcardial perfusion with 4 % paraformaldehyde in PBS. After removal of the brain and overnight postfixation, 50 µm coronal sections were made using a vibratome (Microm, Walldorf, Germany). For immunofluorescent staining, floating sections were washed and incubated overnight with antibodies raised against GFP (chicken, 1:1,000, Aves Labs, Tigard, Oregon,

USA), CB_2 (rabbit, 1:1,000, Cayman Chemical) and CD68 (mouse, 1:2,000, Chemicon, Millipore, Brussels, Belgium) in 10 % donkey serum. After washing the sections were incubated for 2 h with fluorescently labeled donkey anti-chicken antibody (FITC, Jackson Immunoresearch 1:400), donkey anti-mouse (Alexa 555 nm, Invitrogen, merelbeke, Belgium, 1:500) and donkey anti-rabbit (647 nm, Invitrogen, merelbeke, Belgium, 1:500). Finally the cell nuclei were stained with 4',6-diamidino-2-phenylindole (DAPI). Immunofluorescence analysis was done with the AXIO Imager Z1 of Zeiss (Zaventem, Belgium) and the FluoView FV1000 Confocal Microscope of Olympus (Aartselaar, Belgium).

For immunohistochemical analysis sections were treated with 3 % hydrogen peroxide and incubated overnight with the primary rabbit anti-CB_2 antibody (see above) in 10 % donkey serum. The sections were then incubated in biotinylated donkey anti-rabbit secondary antibody, followed by incubation with Strept-ABC-HRP complex (Dako, Glostrup, Denmark). Detection was with diaminobenzidine, using H_2O_2 as a substrate. Analysis was done by light microscopy (Leica DMR). The number of CB_2-positive cells was estimated using the optical fractionator method (Stereoinvestigator software, Microbrightfield, Magdenburg, Germany).

References

1. Valenzano KJ, Tafesse L, Lee G, et al. Pharmacological and pharmacokinetic characterization of the cannabinoid receptor 2 agonist, GW405833, utilizing rodent models of acute and chronic pain, anxiety, ataxia and catalepsy. *Neuropharmacology.* 2005;48:658-672.

2. Larsen P. UJ, Dahlstrom K., Jensen M. Synthesis of [C-11]iodomethane by iodination of [C-11]methane. *Appl Radiat Isotopes.* 1997;48:153-157.

3. Chitneni SK, Garreau L, Cleynhens B, et al. Improved synthesis and metabolic stability analysis of the dopamine transporter ligand [(18)F]FECT. *Nucl Med Biol.* 2008;35:75-82.

4. Fritzberg AR, Whitney WP, Kuni CC, Klingensmith W, 3rd. Biodistribution and renal excretion of 99mTc-N,N'-bis-(Mercaptoacetamido) ethylenediamine. Effect of renal tubular transport inhibitors. *Int J Nucl Med Biol.* 1982;9:79-82.

5. Baekelandt V, Claeys A, Eggermont K, et al. Characterization of lentiviral vector-mediated gene transfer in adult mouse brain. *Hum Gene Ther.* 2002;13:841-853.

6. Liang Q, Gotts J, Satyamurthy N, et al. Noninvasive, repetitive, quantitative measurement of gene expression from a bicistronic message by positron emission tomography, following gene transfer with adenovirus. *Mol Ther.* 2002;6:73-82.

7. Geraerts M, Michiels M, Baekelandt V, Debyser Z, Gijsbers R. Upscaling of lentiviral vector production by tangential flow filtration. *J Gene Med.* 2005;7:1299-1310.

8. Taymans JM, Vandenberghe LH, Haute CV, et al. Comparative analysis of adeno-associated viral vector serotypes 1, 2, 5, 7, and 8 in mouse brain. *Hum Gene Ther.* 2007;18:195-206.

9. Zufferey R, Donello JE, Trono D, Hope TJ. Woodchuck hepatitis virus posttranscriptional regulatory element enhances expression of transgenes delivered by retroviral vectors. *J Virol.* 1999;73:2886-2892.

10. Ibrahimi A, Vande Velde G, Reumers V, et al. Highly efficient multicistronic lentiviral vectors with peptide 2A sequences. *Hum Gene Ther.* 2009;20:845-860.

11. Szymczak AL, Vignali DA. Development of 2A peptide-based strategies in the design of multicistronic vectors. *Expert Opin Biol Ther.* 2005;5:627-638.

Supplemental Table 1. Biodistribution of [^{11}C]GW405833 in NMRI mice

Organ	% Injected Dose ± SD[1]				Standard uptake value ± SD[2]			
	2 min	10 min	30 min	60 min	2 min	10 min	30 min	60 min
Kidneys	10.5 ± 2.2	4.8 ± 0.9	2.3 ± 0.2	1.7 ± 0.2	6.0 ± 0.6	2.8 ± 0.5	1.4 ± 0.2	1.0 ± 0.2
Urine	0.1 ± 0.1	0.2 ± 0.1	0.5 ± 0.1	0.7 ± 0.6	-	-	-	-
Liver	32.4 ± 0.8	40.5 ± 4.1	43.2 ± 0.6	26.7 ± 2.0	6.3 ± 0.5	8.0 ± 0.7	8.3 ± 0.8	5.5 ± 0.6
Spleen	1.0 ± 0.2	0.5 ± 0.1	0.3 ± 0.0	0.2 ± 0.0	2.5 ± 0.7	1.4 ± 0.3	0.8 ± 0.1	0.4 ± 0.1
Pancreas	1.0 ± 0.2	0.9 ± 0.2	0.5 ± 0.1	0.3 ± 0.1	1.9 ± 0.4	1.6 ± 0.3	0.8 ± 0.0	0.5 ± 0.1
Lungs	4.5 ± 0.6	2.4 ± 0.3	1.0 ± 0.4	0.3 ± 0.0	6.7 ± 1.6	3.5 ± 0.3	1.2 ± 0.4	0.5 ± 0.1
Heart	1.9 ± 0.5	0.5 ± 0.3	0.2 ± 0.1	0.1 ± 0.0	3.8 ± 1.0	1.0 ± 0.2	0.5 ± 0.1	0.3 ± 0.0
Intestines	10.2 ± 0.8	12.5 ± 2.3	18.1 ± 2.6	49.6 ± 2.6	-	-	-	-
Stomach	1.8 ± 0.3	2.3 ± 0.6	2.9 ± 1.0	2.0 ± 0.3	-	-	-	-
Blood	3.4 ± 0.6	1.8 ± 0.2	1.7 ± 0.2	1.8 ± 0.1	0.5 ± 0.1	0.3 ± 0.0	0.3 ± 0.0	0.3 ± 0.0
Brain	1.4 ± 0.3	1.0 ± 0.2	0.5 ± 0.0	0.1 ± 0.0	1.4 ± 0.3	1.0 ± 0.1	0.5 ± 0.1	0.3 ± 0.1

Data are expressed as mean ± SD for 4 independent experiments; [1]Percentage of injected dose calculated as cpm in organ/total cpm recovered; [2]Standard uptake values calculated as (radioactivity in cpm in organ/weight of the organ in g)/(total counts recovered/body weight in g)

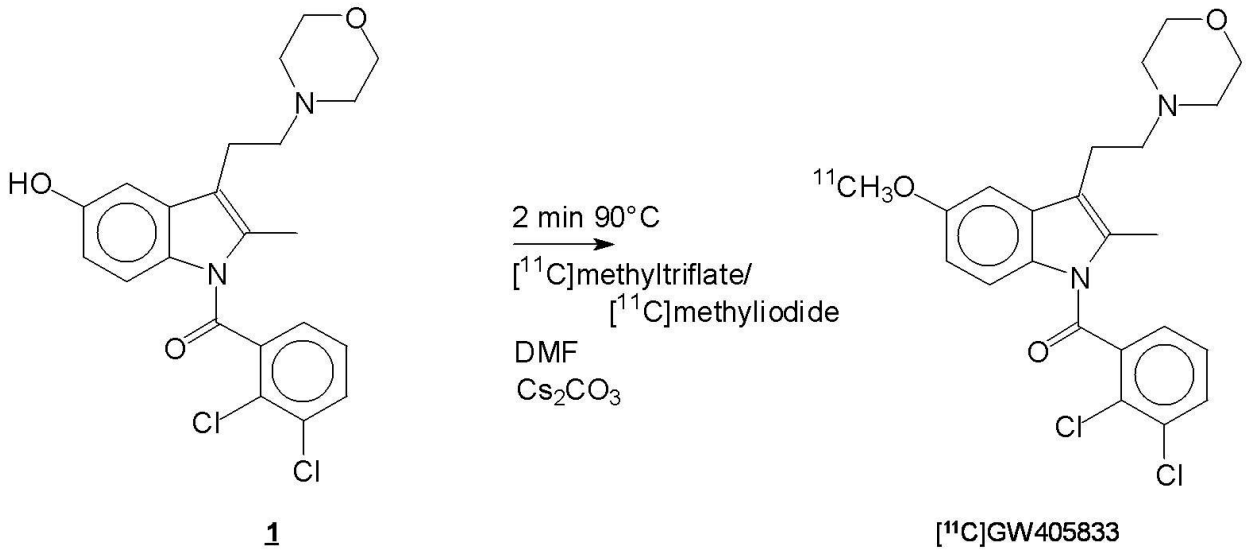

1 **[11C]GW405833**

Supplemental Figure 1. Radiosynthesis of [^{11}C]GW405833

Radiosynthesis of [^{11}C]GW405833 was performed by bubbling [^{11}C]CH_3I or [^{11}C]methyl triflate through a solution of **1** in DMF in basic conditions followed by semi-preparative HPLC purification.

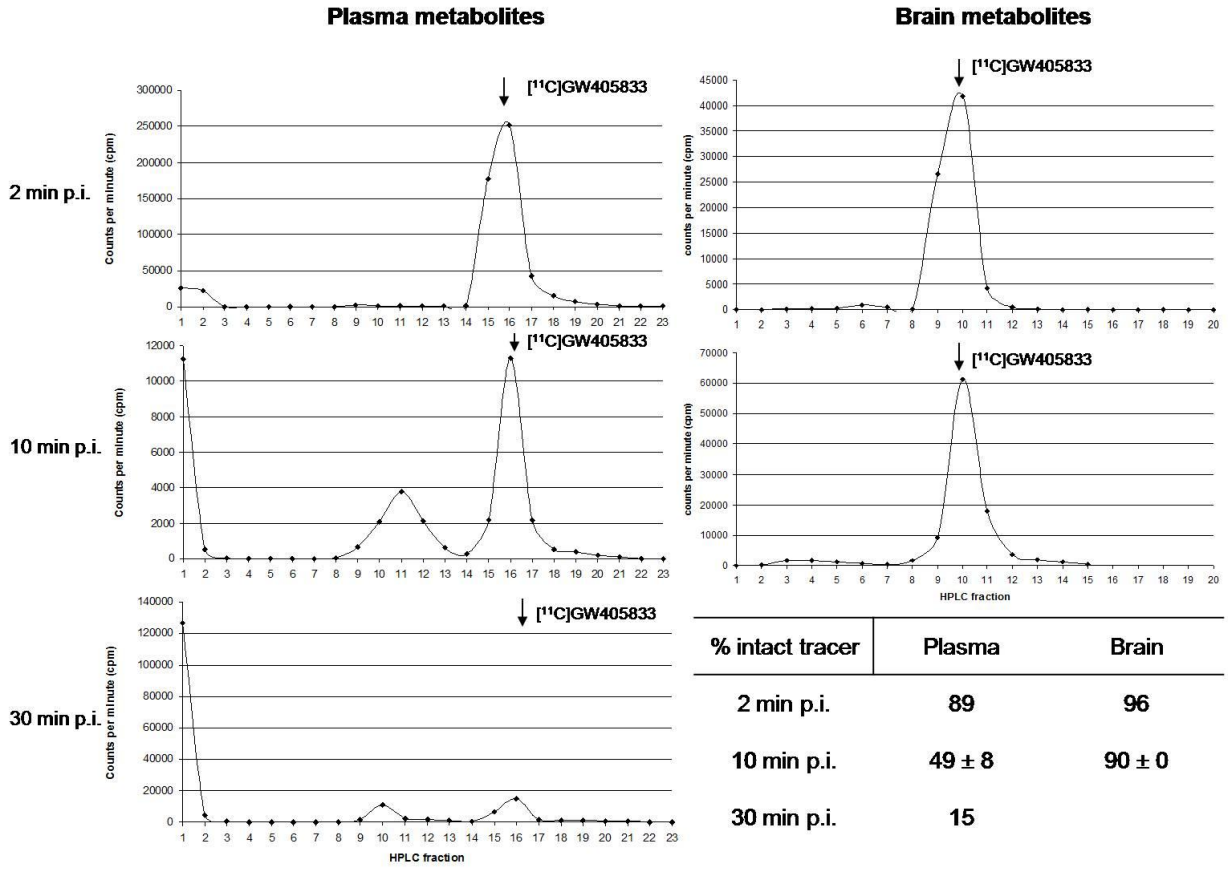

% intact tracer	Plasma	Brain
2 min p.i.	89	96
10 min p.i.	49 ± 8	90 ± 0
30 min p.i.	15	

Supplemental Figure 2. Plasma and brain metabolite analysis of [^{11}C]GW405833 in mice.

The *in vivo* metabolic stability of [^{11}C]GW405833 in plasma and brain was studied in male NMRI mice 2 (n=1), 10 (n=4) or 30 (n=1) min after tracer injection; HPLC analysis reveals the percentage of intact tracer.

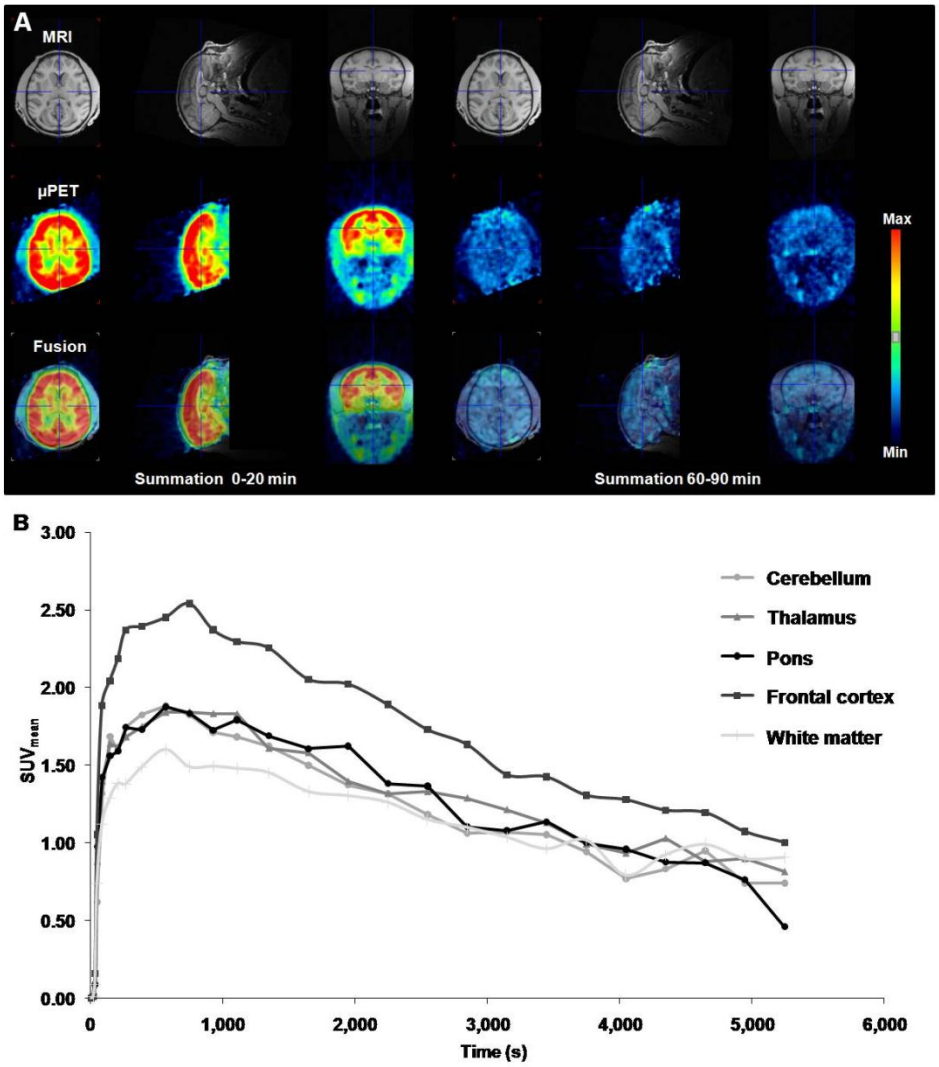

Supplemental Figure 3. The CB_2 radioligand [^{11}C]GW405833 crosses the intact BBB of a rhesus monkey. μPET imaging in a rhesus monkey was performed to investigate the brain uptake of [^{11}C]GW405833. (A) Early (summation 0-20 min) and late frame (summation 60-90 min) rhesus monkey μPET image. Shown are MRI images (upper line), PET images (second line) and a fused image (third line) of the brain of a rhesus monkey after injection of 122 MBq [^{11}C]GW405833. (B) Time-activity curve in different brain regions after injection of [^{11}C]GW405833 in a rhesus monkey.

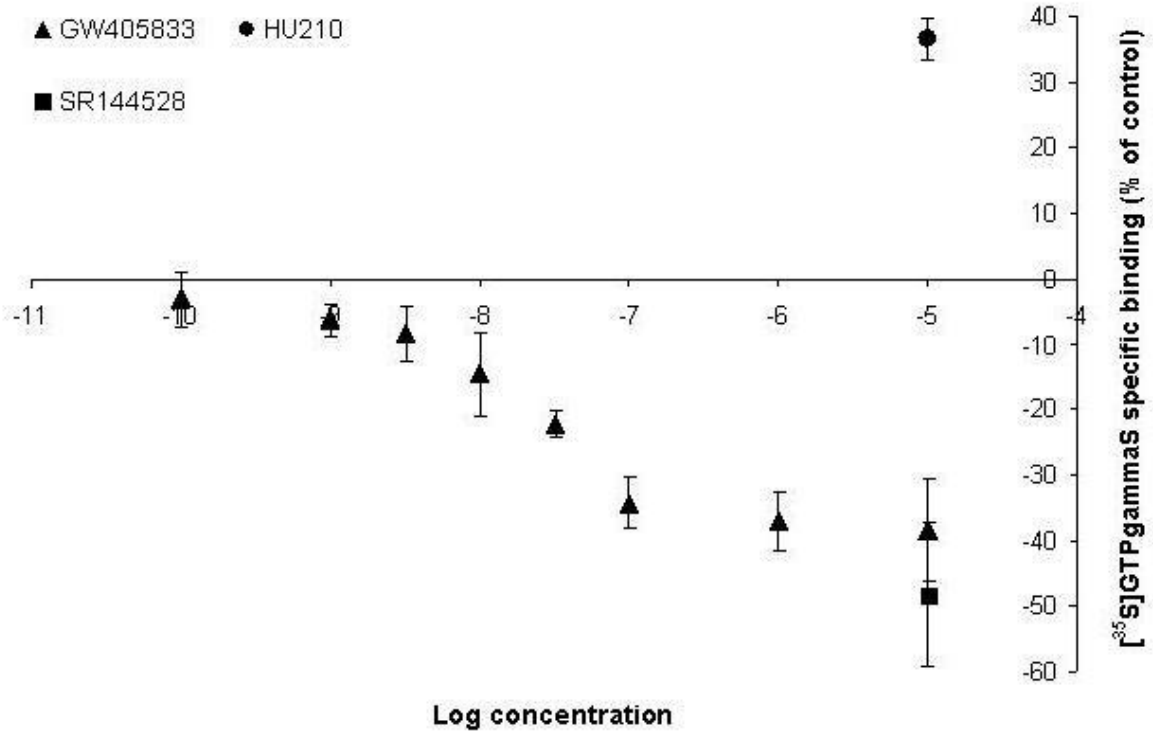

Supplemental Figure 4. Inverse agonistic behaviour of GW405833 in a [^{35}S]-GTPγS assay.

A [^{35}S]-GTPγS assay was used to determine the compounds' intrinsic activity and potency. Effect of HU210 (10 µM, full CB_2 agonist, E_{max} = 36 % relative to basal specific [^{35}S]-GTPγS binding), SR144528 (10 µM, inverse CB_2 agonist, E_{max} = - 48 % relative to basal specific [^{35}S]-GTPγS binding) and GW405833 (full dose-response, E_{max} = - 38 % relative to basal specific [^{35}S]-GTPγS binding) on [^{35}S]-GTPγS binding to CHO cell membranes expressing hCB_2. Mean values of three separate experiments each performed in duplicate are shown; the standard deviation is given by vertical lines.

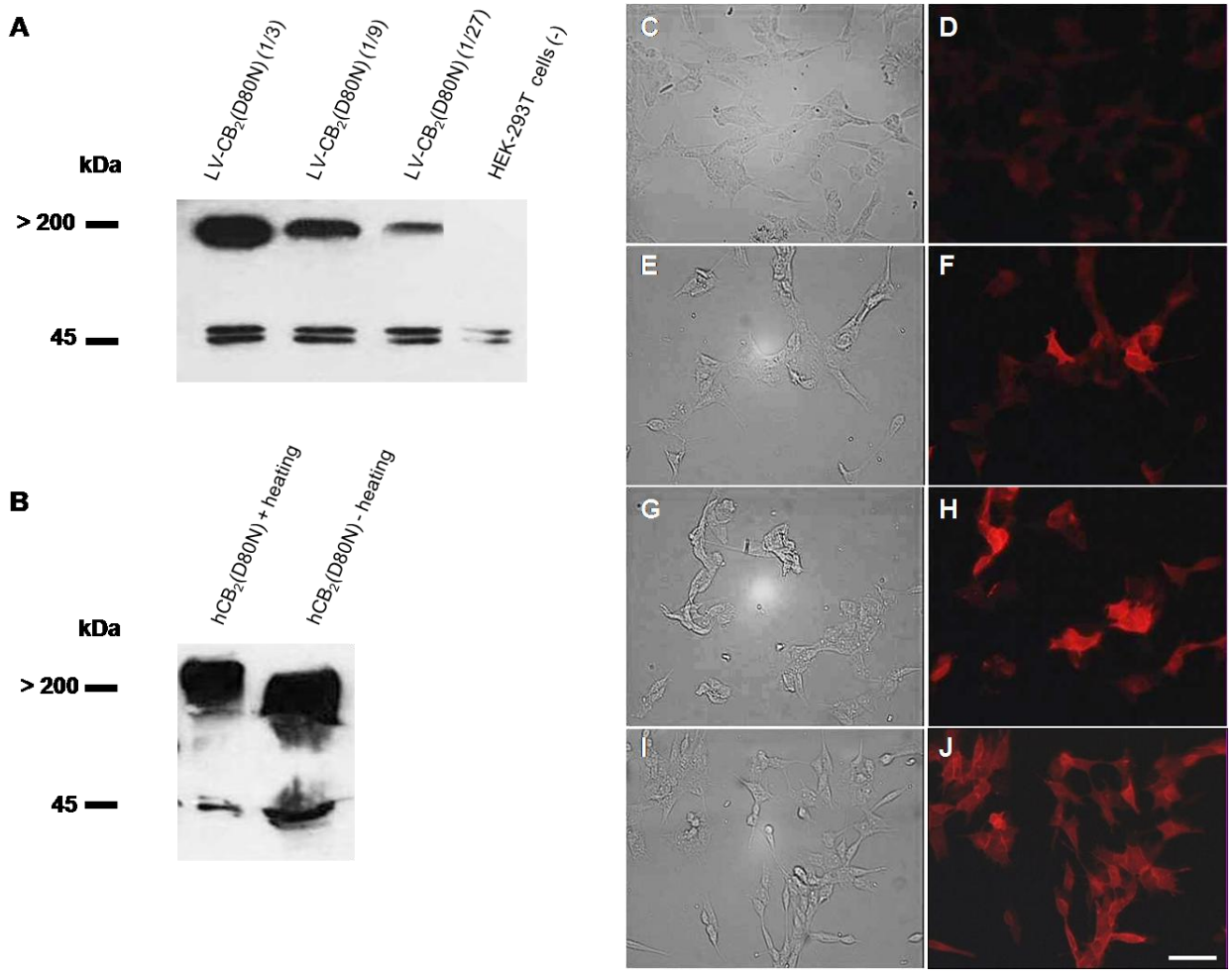

Supplemental Figure 5. (A,B) Western blot analysis of LV-transduced cells. HEK-293T cells transduced with various dilutions of LV-hCB_2(D80N) were subjected to Western blot analysis. HEK-293T lysate was used as negative control. Three CB_2 protein species can be evidenced; proteins of ~40 kDA and ~45 kDa represent non-glycosylated and glycosylated versions of CB_2, respectively, while > 200 kDa species represent CB_2 aggregates due to heating previous to SDS page (A). In (B) the first lane represents CB_2 aggregates after heating of the sample for 1 min at 100 °C. The second sample was loaded without heating. (C-J) **Immunocytochemistry of hCB_2(D80N) expression in cell culture after LV transduction.** SHSY5Y cells were transduced with (C,D) LV-IRES-eGFP, (E,F) LV-hCB_2(D80N), (G,H) LV-

hCB$_2$(D80N)-IRES-eGFP or (I,J) LV-hCB$_2$(D80N)-IRES-Hygro. Cells were stained with a polyclonal Ab against CB$_2$ (visual light C,E,G,I; fluorescence D,F,H,J). CB$_2$ expression was detected in all transduced cell lines except for the cell line transduced with LV-IRES-eGFP. Scale bar = 50 µm

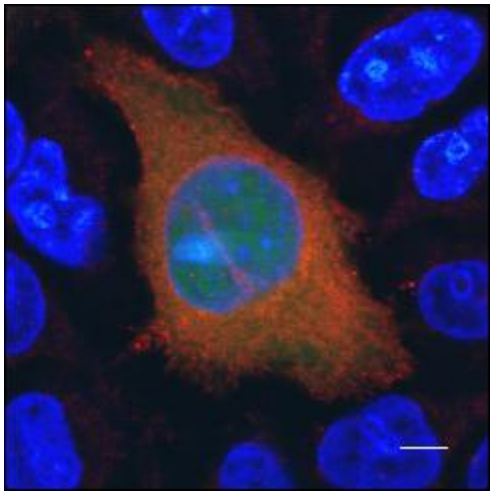

Supplemental Figure 6. Immunocytochemical analysis of hCB$_2$(D80N expression in cell culture after transient transfection. SHSY5Y cells were co-transfected with hCB$_2$(D80N) and eGFP. Cells were plated at 200,000 cells, stained with a polyclonal Ab against CB$_2$ and a Alexa 555 (red) labeled secondary Ab. The cell nuclei were stained with DAPI. Scale bar= 6 µm

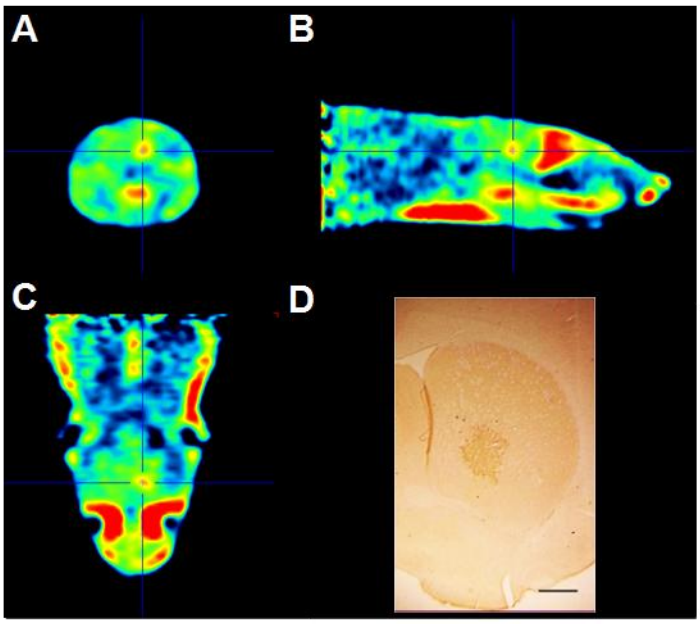

Volume of interest	Uptake (kBq/cc)
Right striatum	51±2
Left striatum	42±1

Supplemental Figure 7. µPET imaging of LV-mediated hCB$_2$(D80N) reporter gene expression in rat brain. 1 week after stereotactic injection of 7.8E+03 pg p24 LV-hCB$_2$(D80N) in the right striatum and 10 min after injection of [^{11}C]GW405833 a 20 min µPET scan was performed. Uptake in right striatum (LV-hCB$_2$(D80N)) is higher than uptake in left striatum (A-C). (D) 9 days after striatal delivery of 7.8E+03 pg p24 LV encoding hCB$_2$(D80N) this rat was sacrificed. Immunohistochemical staining for CB$_2$ on coronal sections shows expression of CB$_2$ in the right striatum. Scale bar = 1 mm